Power Coordination and Line Loss Optimization Strategy of Advanced Traction Power Supply System based on Improved Droop Control

Yalei Wang[1], Li Zeng[1], Jingying Lin[1], and Xiaoqiong He[1,2]

[1] School of Electrical Engineering, Southwest Jiaotong University, Chengdu, China

[2] National Rail Transit Electrification and Automation Engineering Technology Research Center, Southwest Jiaotong University, Chengdu, China

Abstract-- **This paper presents an improved droop control strategy for the advanced traction power supply system (ATPSS). First, we present the ATPSS, whose main feature is the elimination of the neutral sections, which connects the entire AC traction network of the traction power supply system. We also analyze the characteristics of this system compared with other isolated grids. Fluctuations in load position will lead to frequency deviation and power coordination problems. Then, an improved droop control strategy for frequency recovery and reactive power optimization based on multilevel control is proposed. Frequency and reactive power correction signals are sent from the central controller to each traction substation. To reduce line loss, a minimum line loss curve is obtained based on the relationship between active power and line loss, and the active power distribution is adjusted by secondary control. Finally, simulation and experimental results are given to validate the proposed control strategy, which optimizes power coordination, recover system frequency, and reduce line loss.**

*Index Terms—*ATPSS, Droop control, Line Loss Optimization, Power Coordination.

I. INTRODUCTION

The traditional power supply system transformer takes power from the three-phase 110 kV grid and outputs single-phase power to the load. The two power supply arms of the traction substation in the system are α and β phases. Due to the unbalanced load, the voltage phase and amplitude of the supply arms are different. Therefore, the neutral sections need to be set between the different supply arms, which reduces the power supply capacity and restricts the development of trains towards high speed and heavy load.

The ATPSS is the development trend of the traction power supply system, which eliminates the neutral sections and links all the traction networks of traction substations [1]. This system uses an input step-down and output step-up structure but suffers from a lack of capacity. Therefore, a traction power supply system has been proposed that eliminates the step-up transformer, which not only increases the capacity but also reduces the level of withstand voltage required for switches [2]. The structure of ATPSS based on a three-phase to single-phase converter, which outputs a stable and controlled voltage, is shown in Fig.1. As the input and output of the converter need to be connected to the high voltage grid, a multi-winding step-down transformer and a cascade structure are used on them respectively. Therefore, the grid connection of advanced traction substations is equivalent to several cascaded inverters connected to the AC traction network.

Advanced traction substations are connected to the AC traction network, which forms an islanded grid consisting of voltage source inverters. As shown in Fig.1, the traction load is connected to the AC traction network. The main objectives of the system are to coordinate the output power of the traction substation, to correct the frequency deviations, and to save energy. Many scholars have studied similar problems in the context of microgrid [3, 4]. To solve the power coordination problem in AC grids, a power decoupling technique has been proposed [5]. An orthogonal linear rotational transformation matrix has been proposed to correct active and reactive power [6]. The line impedance of ATPSS is dynamic and the load position is variable, so the above methods are not applicable. Therefore, based on the known train position, the secondary control adjusts the parameters of the system to achieve the established control objectives.
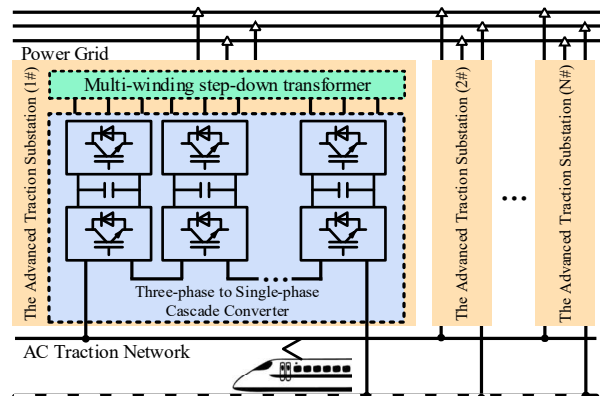

Fig. 1: Structure of ATPSS

II. Adjustment Of Droop Characteristics By The Secondary Control

The proposed improved droop control strategy in this paper is achieved through secondary control, which not only optimizes the power output of the traction substation but also recovers the system frequency and reduces the line loss.

A. Analysis of droop characteristics

Based on local control, we can adjust the droop control parameters of the cascaded converter by exchanging signals with the secondary controller, as shown in Fig. 2.
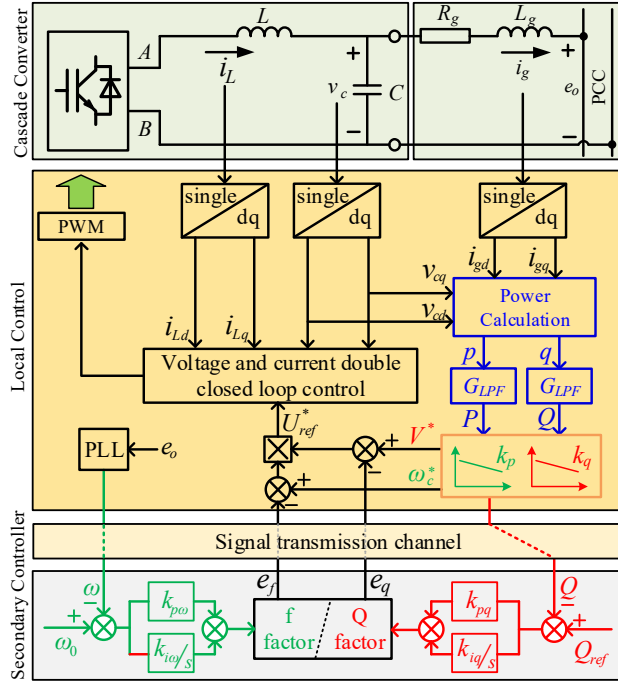

Fig. 2: Control strategy and topology of cascade converter

The local control is based on three control loops- a power control outer loop based on the droop characteristic curve and a double closed loop for voltage and current to output a stable voltage and improve the dynamic response speed.

In the power control outer loop, capacitor voltage v_c and output current i_g calculate the instantaneous power p and q. According to the droop characteristic, we can calculate the reference voltage for the inner loop control from P and Q, which includes voltage amplitude V^* and angular frequency ω_c^*. With the internal loop control, the inverter will output a stable voltage in amplitude and phase without considering the correction of the droop characteristics by the secondary control. In local control, we control the voltage amplitude and phase to output the given power. The principle is as follows:

Assuming the capacitor voltage v_c and grid-connected point voltage e_0 do not contain harmonics, the voltages can be respectively expressed as

$$\begin{cases} v_c(t) = U\cos(\omega t + \delta) \\ e_0(t) = E\cos(\omega t) \end{cases} \tag{1}$$

The relationship between P, Q, and U, δ can be obtained through transmission power calculation as

$$\begin{aligned} P &= \frac{R_g}{R_g^2 + (\omega L_g)^2}\left(U^2 - EU\cos\delta\right) \\ &+ \frac{\omega L_g}{R_g^2 + (\omega L_g)^2}EU\sin\delta \\ Q &= \frac{R_g}{R_g^2 + (\omega L_g)^2}\left(U^2 - EU\cos\delta\right) \\ &- \frac{\omega L_g}{R_g^2 + (\omega L_g)^2}EU\sin\delta \end{aligned} \tag{2}$$

where R_g and L_g are resistance and inductance from the inverter to the grid-connected point. Using perturbation analysis, the perturbation equation can be obtained, which is expressed as

$$\begin{cases} \hat{P} = \dfrac{\omega L_g U^2}{R_g^2 + (\omega L_g)^2}\hat{\delta} \\ \hat{Q} = \dfrac{\omega L_g U}{R_g^2 + (\omega L_g)^2}\hat{U} \end{cases} \tag{3}$$

where $\hat{P}$, $\hat{Q}$, $\hat{U}$, $\hat{\delta}$ are perturbations of P, Q, U, δ respectively.

In general, ω, which has a differential relationship with δ, is selected as the control object. The droop control equation is

$$\begin{cases} \omega - \omega_0 = -k_p(P - P_0) \\ U - U_0 = -k_q(Q - Q_0) \end{cases} \tag{4}$$

$$\xrightarrow[U^* = -k_q Q_0 + U_0]{\omega^* = -k_p P_0 + \omega_0} \begin{cases} \omega = \omega^* - k_p P \\ U = U^* - k_q Q \end{cases}$$

B. Regulation function of secondary control

The structure of the secondary control is shown in Fig. 2 and Fig. 3.

In P-f droop control, the active power shortage causes the traction network frequency to deviate from the reference value. The main purpose of P-f secondary control is to achieve the system frequency recovery through active power coordination. Since the droop parameter of the cascaded inverters in droop control is usually the inverse ratio of the rated capacity, the P-f droop parameters are the same for the traction substations with the same rated capacity. Furthermore, considering that frequency is the global variable in the ATPSS, the frequency recovery process is unified with the active power coordination in the secondary control. This paper first describes the frequency recovery process. A centralized control structure is used to realize the P-f secondary control.
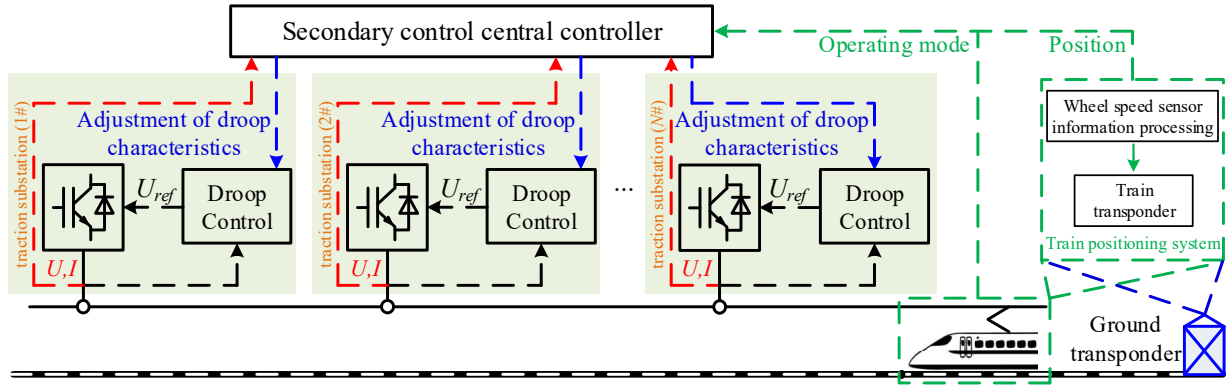
Fig. 3: Structure of secondary control information transmission

The implementation process of the secondary controller is shown in Fig. 2.

By using a phase-locked loop (PLL) for the system voltage, we obtain the system angular frequency ω. ω is compared with the reference angular frequency ω^* in the secondary controller, and then the active power shortage e_{fs} is generated by the PI controller. e_{fs} is assigned as e_{f1}, e_{f2}, e_{f3}, etc. according to the power participation factor of each traction substation. The calculation process is

$$e_{fi} = k_i(k_{p\omega} + {k_{i\omega}}/{s})(\omega - \omega_0) \tag{5}$$

where k_i is the power participation factor of the traction substation, and $k_{p\omega}$ and $k_{i\omega}$ are the PI parameters of the secondary controller. e_{fi} is sent to each traction substation through the signal transmission channel. The principle of frequency recovery control is shown in Fig. 4(a).

a)Frequency recovery control

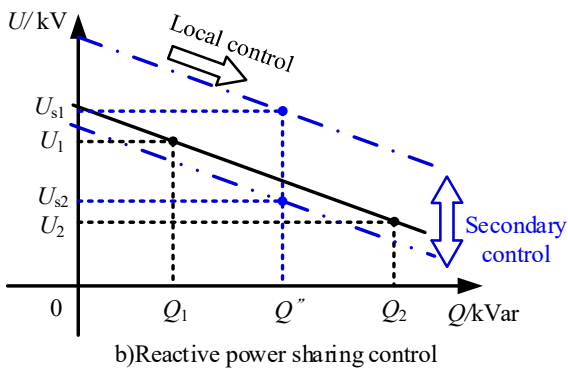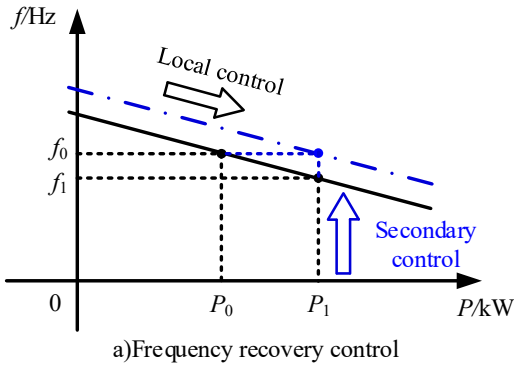

b)Reactive power sharing control

Fig. 4: Process of frequency recovery and reactive power distribution

In the case of traction substations connected to the AC traction network, the line impedance and train load are the major factors affecting the reactive power distribution. We collect the reactive power output of each traction substation and obtain the secondary voltage control variable e_{qi} after processing by the central controller.

$$\begin{cases} Q_{refi} = Q_{mi}\dfrac{Q_{load}}{\displaystyle\sum_{i=1}^{n}Q_{mi}} \\ e_{qi} = (k_{pq} + {k_{pi}}/{s})(Q_{refi} - Q_i) \end{cases} \tag{6}$$

where Q_{refi} is the reactive power reference value of the traction substation, k_{pq} and k_{iq} are the PI parameters of secondary reactive power control, Q_{mi} is the maximum reactive power that can be output by the cascade inverter, Q_{load} is the total reactive power of the line and the train. The principle of reactive power distribution control is shown in Fig. 4(b).

As shown in Fig. 5, two traction substations provide power for one traction load. The power flow direction is that two traction substations generate power and the train absorbs power. Ignoring the admittance of the line to the ground, the active power line loss is

$$\Delta P = \Delta P_1 + \Delta P_2$$
$$= \frac{1}{U_L^2}\Big[\big(P_1^2 + Q_1^2\big)R_1 + \big(P_2^2 + Q_2^2\big)R_2\Big] \tag{7}$$

Under the condition of reactive power sharing, (7) is a bivariate function related to P_1 and R_1. Assuming that the total transmitted power and line resistance of the AC traction network are fixed values, Fig. 6 plots the relationship between the line loss ΔP and output power P_1, line resistance $R1$. According to the minimum loss curve, to minimize the total loss of the line, the output power of the traction substation near the train should be larger.

R_1 can be calculated from the position signal of the train. The secondary controller sends the active power reference P_{refi} to each traction substation according to the line loss minimum curve. Therefore, when the train moves between two traction substations, we can adjust the active power reference to achieve the minimum line loss.
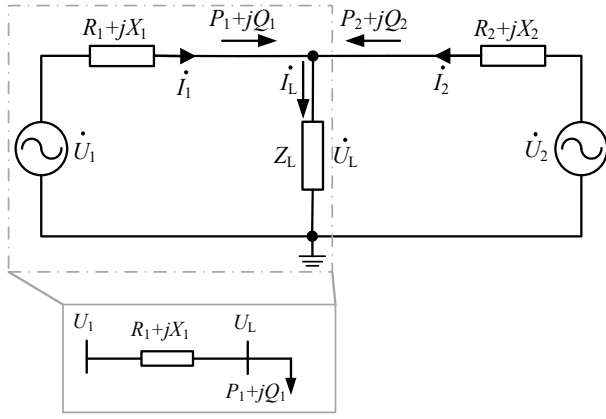
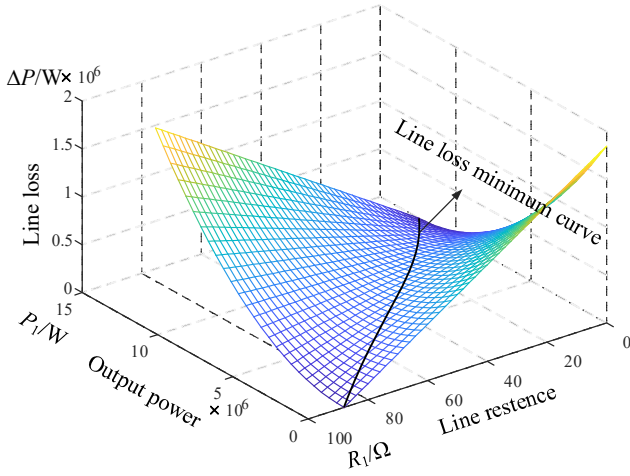Fig. 5: Structure of bilateral power supply

Fig. 6: Line loss minimum curve

III. SIMULATION AND EXPERIMENTAL VERIFICATION

The simulation model is built in MATLAB/Simulink according to the topology as shown in Fig.7 and the parameters are listed in Table I. The train is simulated in the Simulink as it travels from substation 2 to substation 1. The cascaded inverter adopts a single-phase three-level topology, and the LC filter at the output side filters out the high-frequency harmonics generated by the switch.
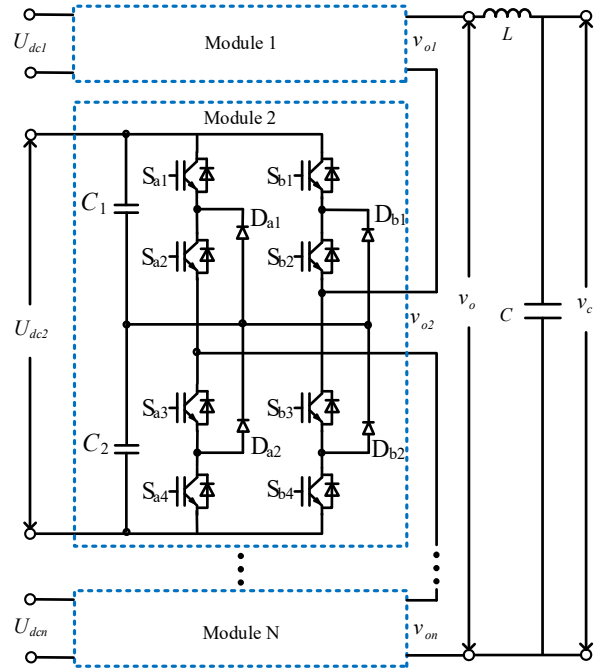

Fig. 7: Cascade inverter topology

TABLE I
THE SIMULATION PARAMETERS OF CASCADE CONVERTER

Name	Value
Power grid voltage RMS	110kV
AC traction grid voltage RMS	27.5kV
DC voltage, u_{dci}	4kV
DC-link capacitance, C_i	8mF
LC filter, L/C	5mH/4mF
Switching frequency	3kHz

The comparison and analysis of output power, frequency and line loss under different control strategies are as follows:
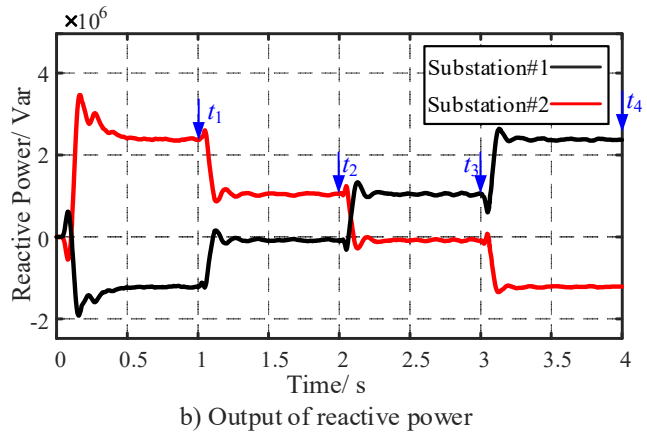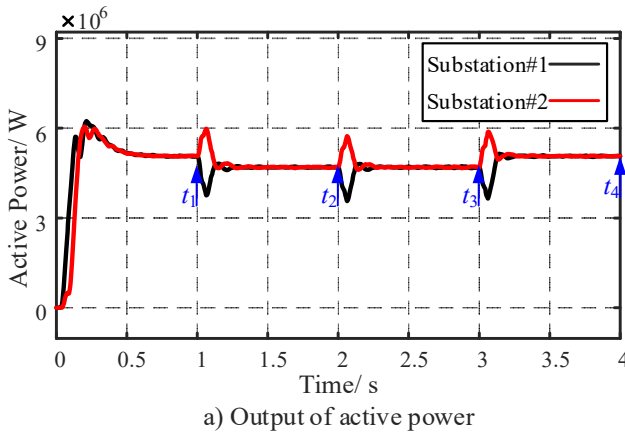

a) Output of active power

b) Output of reactive power

Fig. 8: Power output results of traditional control strategy

a) Frequency restoration

b) Reactive power sharing
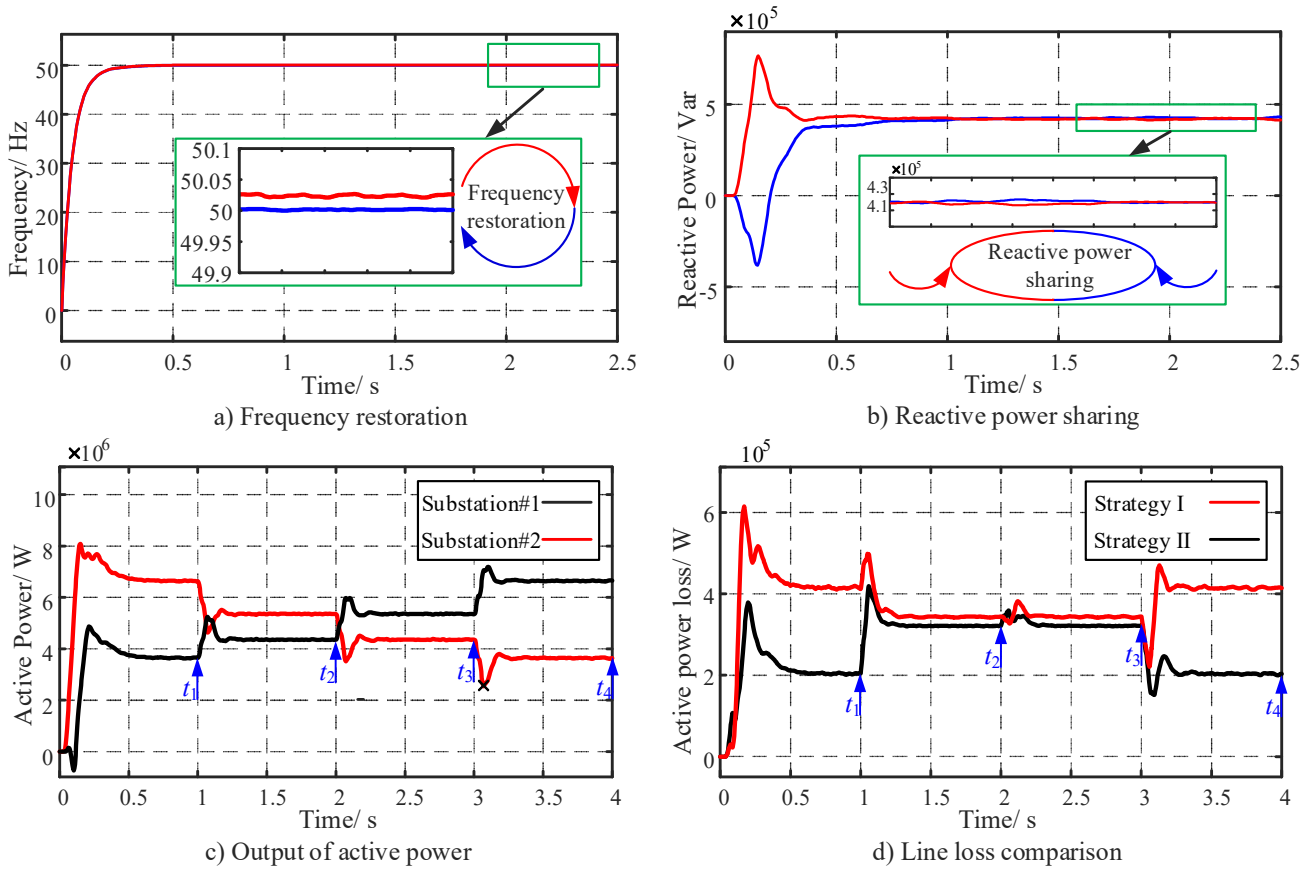
c) Output of active power

d) Line loss comparison

Fig. 9: Simulation results of proposed improved droop control strategy

Control strategy I: Traditional droop control. As shown in Fig. 8, the train position is switched every 1 second from the moment t_1 to simulate the process of the train from substation 2 to substation 1. In this strategy, we do not use secondary control, so the droop characteristics of the substation are the same. The active power output of both substations is the same and the reactive power output is naturally distributed. From Fig. 8(a), we know that the train is closer to substation 2 from 0 to t_1, and the system starts smoothly. Since the power of the two substations is the same, the line loss is larger and the total output power is higher. At the moment t_1, the train starts to move away from substation 2 and the active power output quickly returns to stability and remains at the same value. At moments t_2 to t_4, the train approaches substation 1, and the output power of the two substations is opposite to the trend of 0 to 2 seconds. As shown in Fig. 8(b), the reactive power output by the substation is only related to the position of the train without secondary control. The substation close to the train outputs inductive reactive power, while the substation far away absorbs inductive reactive power.

Control strategy II: Proposed improved droop control. In Fig. 9, we show the simulation results of the proposed control strategy in terms of frequency recovery, reactive power coordination, and line loss reduction.

In Fig. 9(a), we show the output frequency value of voltage PLL for different control strategies. The simulation results show that the proposed control strategy can recover the system frequency to the rated operating frequency-50Hz.

According to Fig. 8(b), the maximum difference in output reactive power is observed when the train is close to the substation. In Fig. 9(b), we show the reactive power output by the substations when the secondary control of reactive power is added. At this time, the train is close to substation 2, which is the most difficult to control the reactive power output. The reactive power output of the two substations gradually tends to be consistent after 1 second of the startup.

From Fig. 6, we get the line loss minimum curve, which provides a reference for the secondary control of active power. As shown in Fig. 9(c) and (d), from t_1 to t_4, the train is closer to substation 2. With the secondary control, we increase the active power reference of substation 2 and decrease the active power reference of substation 1. Depending on the train's location, the substation's output power is different, and the two active power curves in Fig. 9(c) are obtained. Compared with control strategy I, the line loss has been reduced. If the droop characteristics of the substations differ greatly, the system loses stability, so the line loss curve in use is modified from the curve in Fig. 6.

The Rapid Control Platform (RCP) and Hardware-in-loop (HIL) platforms have been designed to verify the proposed control strategy, as shown in Fig. 10. The parameters of the HIL platform are listed in Table II.

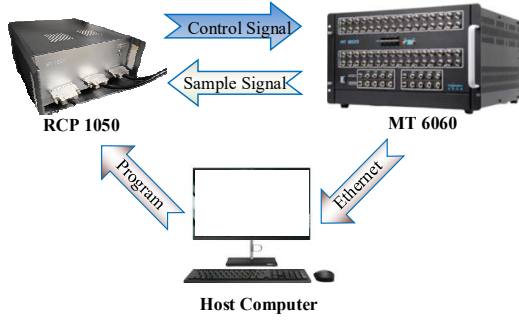| Name	Value
Power grid voltage RMS	1.1kV
AC traction grid voltage RMS	275V
DC voltage, u_{dci}	40V
DC-link capacitance, C_i	470uF
LC filter, L/C	3mH/50uF
Switching frequency	3kHz

Fig. 10: Hardware-in-loop simulation platform

In Fig. 11 and Fig. 12, e_{o1}, e_{o2}, i_{g1}, i_{g2} are the output voltage and output current of substation 1 and substation 2 respectively.
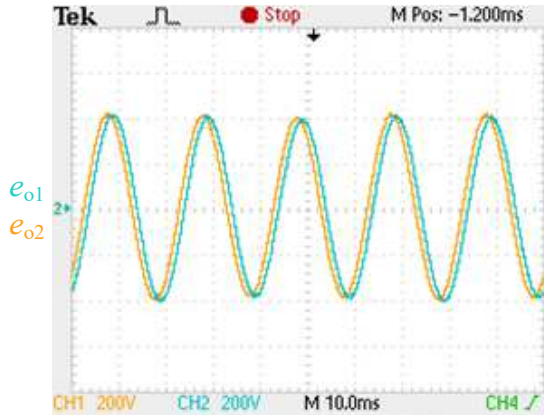

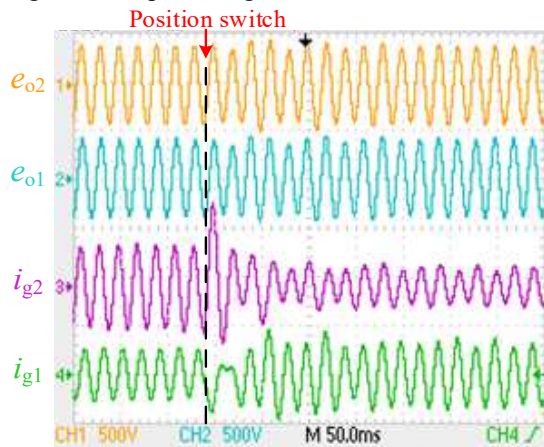Fig. 11: Output voltage of traction substation

Fig. 12: Power output coordination

As shown in Fig. 11, when the output power of traction substation 2 is larger, the output voltage of the two traction substations has an obvious phase difference. It can be proved that the proposed strategy can achieve power output difference by adjusting the output voltage phase angle.
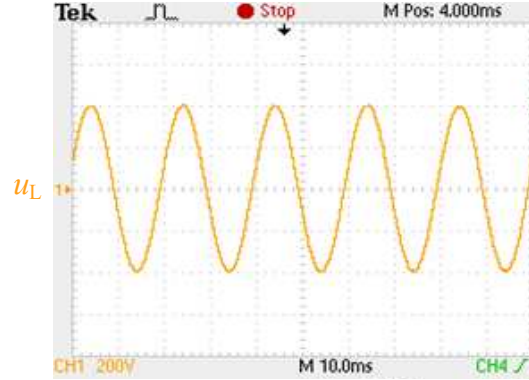

Fig. 13: Train voltage u_L

When the train position is switched, the output currents of the two substations change. Fig. 12 shows that the current in substation 2 decreases and the current in substation 1 increases, but the total output power reduces. Since the voltage at the train remains unchanged, the line loss is reduced. With this platform, the power coordination and line loss optimization strategies are validated.

IV. CONCLUSION

ATPSS has advantages over traditional traction power supply systems, which can realize the overall connection of traction network. The improved droop control strategy proposed in this paper only requires the positioning of trains and relies on secondary control to achieve power coordination control and line loss optimization of ATPSS. This paper proves the effectiveness of the strategy through simulation and experiments.

REFERENCES

[1] X. He, Z. Shu, X. Peng, et al., "Advanced Cophase Traction Power Supply System Based on Three-Phase to Single-Phase Converter," *IEEE Trans. Power Electron*., vol. 29, no. 10, pp. 5323-5333, Oct. 2014.

[2] X. He, P. Han, Y. Wang, et al., "Study on Advanced Cophase Traction Power Substation System Based on Cascade-parallel Converter", *Journal of the China Railway Society*, vol. 39, no. 8, pp. 52-61, Aug. 2017.

[3] P. Han, X. He, H. Ren, et al. Fault Diagnosis and System Reconfiguration Strategy of a Single-Phase Three-Level Neutral-Point-Clamped Cascaded Inverter [J] IEEE Trans. Industry Applications. 2019, 55(4): 3863-3876.

[4] X. Wu, C. Shen, R. Iravani. "A Distributed, Cooperative Frequency and Voltage Control for Microgrids", *IEEE Trans. Smart Grid*, vol. 9, no. 4, pp. 2764-2776, July 2018.

[5] T. Wu, Z. Liu, J. Liu, et al., "A unified virtual power decoupling method for droop-controlled parallel inverters in microgrids," *IEEE Trans. Power Electron*., vol. 31, no. 8, pp. 5587-5603, Aug. 2016.

[6] K. De Brabandere, B. Bolsens, J. Van den Keybus, et al., "A voltage and frequency droop control method for parallel inverters," *IEEE Trans. Power Electron*., vol. 22, no. 4, pp. 1107-1115, Jul. 2007.